scientific reports

Check for updates

OPEN

Validation of circulating miR-323a-3p and miR-625-3p to classify hypertrophic cardiomyopathy in Friedreich's ataxia

José Santiago Ibáñez-Cabellos[1,2,3], Raquel Baviera-Muñoz[4], Berta Alemany-Perna[5], Rafael Sivera[2,6], Luis Bataller[7], Sergio Cesar[8,9], Pilar González-Cabo[1,2,3], José Luis García-Giménez[1,2,3], Federico V. Pallardó[1,2,3]✉ & Marta Seco-Cervera[1,2,3]✉

Friedreich's ataxia (FRDA) is an inherited neurodegenerative disorder frequently complicated by hypertrophic cardiomyopathy (HCM), a major cause of morbidity and mortality in these patients. Conventional protein biomarkers, such as high-sensitivity troponin or collagen turnover markers, provide only modest diagnostic accuracy, highlighting the need for more sensitive tools. Circulating microRNAs (miRNAs) have emerged as promising non-invasive biomarkers, but independent validation in FRDA remains limited. We analyzed a cohort of FRDA patients ($n = 34$) and age-, sex-, and race-matched healthy controls ($n = 34$). Expression of a previously proposed miRNA signature was evaluated in plasma using RT-qPCR, with normalization to miR-16-5p, replicating prior methodology. Echocardiographic parameters were compared across subgroups. Associations between differential miRNA expression, comorbidities (diabetes mellitus, cardiomyopathy), and echocardiographic measures were evaluated. Receiver Operating Characteristic (ROC) curves and multivariable logistic regression assessed diagnostic performance. Five of seven candidate miRNAs were validated as differentially expressed in FRDA compared with controls. Among patients, miR-128-3p, miR-130b-5p, miR-151a-5p, miR-330-3p, and miR-142-3p were significantly up-regulated in those with diabetes. For cardiomyopathy, both miR-323a-3p (previously described by our group) and miR-625-3p showed strong associations. A multivariable model combining miR-323a-3p and miR-625-3p achieved promising discriminative performance for HCM (Area Under the Curve (AUC) = 0.84; sensitivity 80%; specificity 71.4%), outperforming traditional protein biomarkers. This two-miRNA panel offers robust non-invasive prediction of HCM in FRDA and highlights metabolic miRNAs as dual biomarkers for diabetes comorbidity. Prospective longitudinal studies and development of standardized diagnostic kits are warranted to integrate miRNA profiling into FRDA clinical care.

Keywords Epigenetics, FRDA, MiRNAs, Biomarkers, Cardiopathy

Abbreviations

FRDA	Friedreich's ataxia
HCM	Hypertrophic cardiomyopathy
miRNAs	MicroRNAs
IVS	Interventricular septal thickness

[1]Department of Physiology, Medicine and Dentistry School, University of Valencia, Av. Blasco Ibáñez, 15, 46010 Valencia, Spain. [2]Consortium Center for Biomedical Network Research on Rare Diseases (CIBERER), Institute of Health Carlos III, Valencia, Spain. [3]INCLIVA Health Research Institute, INCLIVA, Valencia, Spain. [4]Department of Neurology, Hospital de Manises, Manises, Spain. [5]Unit of Ataxias, Spastic Paraparesis, and Rare Neurological Diseases, Neurology Service, Hospital Universitari de Girona Dr. Josep Trueta (Girona) and Hospital de Santa Caterina (Salt), Girona, Spain. [6]Neuromuscular and Ataxia Diseases Unit, Hospital Universitari i Politècnic La Fe, Valencia, Spain. [7]Department of Neurology, Instituto Valenciano de Oncología, Valencia, Spain. [8]Arrhythmia, Inherited Cardiac Diseases and Sudden Death Unit, Hospital Sant Joan de Déu, Esplugues de Llobregat, Barcelona, Spain. [9]Arrítmies Pediàtriques, Cardiologia Genètica i Mort Sobtada, Malalties Cardiovasculars en el Desenvolupament, Institut de Recerca Sant Joan de Déu (IRSJD), Esplugues de Llobregat, Barcelona, Spain. ✉email: federico.V.Pallardo@uv.es; Marta.seco@uv.es

LVPWT	Posterior wall thickness
LVEDd	Left ventricular end diastolic diameter
LVESd	Left ventricular systolic diameter
LVEF	Left ventricular ejection fraction
RWT	Relative wall thickness

FRDA is a common inherited ataxia, mostly caused by GAA trinucleotide repeat expansions in the first intron of the *FXN* gene, leading to decreased expression of frataxin, a mitochondrial protein essential for iron–sulphur cluster biogenesis and mitochondrial function. Frataxin deficiency results in mitochondrial iron accumulation, oxidative stress, and impaired energy production, contributing to progressive neurodegeneration and multisystemic involvement. Clinically, FRDA typically presents in childhood or adolescence with progressive gait and limb ataxia, dysarthria, loss of deep tendon reflexes, and proprioceptive deficits[1,2]. Other systemic manifestations of FRDA include scoliosis, diabetes, and cardiac abnormalities[3–5]. Importantly, up to two-thirds of patients develop hypertrophic cardiomyopathy, which significantly contributes to disease burden and is the leading cause of premature death in FRDA[6,7].

Given the variability in disease progression and clinical presentation, there is a growing need for reliable biomarkers to monitor disease status and predict organ-specific involvement, particularly cardiac dysfunction. In this context, epigenetic biomarkers, especially miRNAs, have gained attention for their potential as non-invasive indicators of pathological changes[8]. miRNAs are small non-coding RNAs that regulate gene expression post-transcriptionally and are involved in a wide range of cellular processes, including mitochondrial function, oxidative stress response, and cardiac remodelling[9,10]. Altered expression profiles of specific circulating miRNAs have been associated with both neurodegenerative and cardiovascular diseases[11–13], making them attractive candidates for biomarker development in FRDA. Previous studies have identified circulating miRNA signatures associated with multisystem involvement in FRDA[14], including links to pancreatic and neuromuscular dysfunction[15]. More recently, combined miRNA panels have shown prognostic potential, although without incorporating cardiac phenotyping[16]. Their stability in body fluids and the availability of sensitive detection methods further support their clinical applicability[17–19]. Exploring miRNA signatures in FRDA may thus offer new insights into disease mechanisms and help identify early predictors of cardiomyopathy in this vulnerable patient population.

In this study, we aim to confirm a microRNA panel previously identified by our group[8] and further assess the potential of miR-323a-3p as a biomarker for cardiomyopathy in FRDA patients. The validation of this microRNA signature, with particular focus on miR-323a-3p, could provide a valuable tool for the early detection of cardiac involvement and facilitate risk stratification, ultimately contributing to improved clinical management of these patients.

Methods

Study design and population

The study cohort consisted of genetically confirmed FRDA patients from unrelated families. Patients were recruited at Hospital Universitario y Politécnico La Fe (Valencia) and Hospital Universitari de Girona Dr. Josep Trueta (Girona), in collaboration with the Neurology and Cardiology departments. Individuals with active infections or neoplastic conditions at the time of recruitment were excluded. Clinical, demographic, and echocardiographic data were retrospectively extracted from patients' electronic medical records, including age, sex, history of diabetes and cardiomyopathy, current medications and therapies, number of GAA repeat expansions, and disease duration. Of the 34 FRDA patients, cardiac phenotyping was performed using the most recent echocardiogram available within 18 months before or after blood sampling ($n = 32$). Two patients whose last echocardiogram, showing no evidence of cardiomyopathy, had been performed 6–8 years prior to blood sampling were excluded from cardiac phenotype analyses due to the uncertainty of their current cardiomyopathy status, but were retained in all other comparisons (FRDA vs. controls and diabetes stratification). In this study, information from transthoracic echocardiography included measurements of interventricular septal thickness (IVS), posterior wall thickness (LVPWT), left ventricular end-diastolic diameter (LVEDd), left ventricular end-systolic diameter (LVESd), and left ventricular ejection fraction (LVEF). The collected samples were incorporated into a public repository for FRDA within the CIBERER Biobank (www.ciberer-biobank.es), ensuring availability for future research purposes. Healthy volunteers with no neoplastic diseases, active infection, cardiomyopathy, heart problems, hypertension, or diabetes were enrolled by the INCLIVA Biobank and CIBERER Biobank. The participants of both groups (healthy volunteers and FRDA patients) were matched by race, sex and age and were processed in the same way.

Experimental protocols and methods were carried out after obtaining approval from the Biomedical Research Ethics Committee of HCUV (2022/173) and RVB (RVB21041ER) and it were conducted in accordance with the Declaration of Helsinki. All participants or their legal guardians provided written informed consent prior to inclusion.

Echocardiographic parameters

The echocardiographic parameters analyzed included IVS, defined as the distance between the endocardial borders of the interventricular septum at end-diastole; LVPWT, measured perpendicularly to the long axis of the left ventricle at end-diastole; LVEDd and LVESd corresponding to the internal cavity size at end-diastole and end-systole, respectively; LVEF was calculated as the percentage of blood volume ejected from the left ventricle during each cardiac cycle. Relative Wall Thickness (RWT) was obtained using the following equation: 2*LVPWT/LVEDd[20,21].

Given the retrospective design of the study, it was assumed that all participating centers adhered to standard echocardiographic acquisition protocols recommended by the European Association of Cardiovascular Imaging and the American Society of Echocardiography. Calculation of LVEF was preferentially performed using the Simpson's biplane method, in accordance with current recommendations[20,21].

The diagnosis of hypertrophic cardiomyopathy was established using validated electrocardiographic and echocardiographic criteria adapted for the FRDA context. Echocardiographic assessment was the primary diagnostic criterion. Left ventricular posterior wall thickness (LVPWT) was measured in the parasternal long-axis view[20], and a value > 11 mm was considered diagnostic of HCM. Patients meeting this threshold were classified as having cardiomyopathy. In borderline cases, defined as LVPWT values of 10 mm, additional parameters were considered. Specifically, the presence of interventricular septal thickness (IVS) > 11 mm together with electrocardiographic criteria of left ventricular hypertrophy was required to establish the diagnosis of HCM. Electrocardiographic evaluation included calculation of the Cornell voltage index (sum of the R wave amplitude in lead V3 and the S wave amplitude in lead aVL), with values > 28 mm in men and > 20 mm in women considered indicative of left ventricular hypertrophy[22]. Electrocardiographic findings were not used in isolation but contributed to the diagnostic classification only in the context of borderline echocardiographic measurements, as described above. Accordingly, the diagnosis of HCM used for subsequent analyses, including ROC curve evaluation, was based on a combination of echocardiographic criteria, with ECG findings applied only in predefined borderline cases. For descriptive analyses of echocardiographic parameters (IVS, LVEDd, LVESd, LVEF, and RWT), each variable was analyzed using all FRDA patients with available measurements; patients with missing data for a given parameter were excluded only from the corresponding analysis, resulting in variable sample sizes across analyses.

A limitation of this study is that both ECG and echocardiographic data were collected retrospectively from routine clinical records. Consequently, detailed information regarding equipment models, imaging settings, and operator-specific protocols was not consistently available. To minimize potential variability, only examinations interpreted by board-certified cardiologists were included, and values were extracted directly from the final clinical reports.

RNA extraction and quantification

Peripheral blood was drawn from both FRDA patients and control subjects. To obtain plasma, samples underwent an initial centrifugation at 2500 rpm for 10 min, followed by a second centrifugation step at 16,000 × g for 10 min at 4 °C. Plasma aliquots were stored at − 80 °C until RNA extraction.

For RNA isolation, 200 µL of plasma per sample were processed using the miRNeasy Serum/Plasma kit (Qiagen, Valencia, CA, USA) according to the manufacturer's instructions. The final RNA was eluted in 25 µL of RNase-free water. Quantification of total RNA, including miRNAs, was performed with the NanoDrop™ One Microvolume UV-Vis Spectrophotometer (Thermo Scientific, Waltham, MA, USA).

Real-time qPCR validation of miRNA

Circulating miRNAs were quantified following the methodology previously[8]. Briefly, reverse transcription was performed using the TaqMan™ MicroRNA Reverse Transcription Kit and miRNA-specific stem-loop primers (Part No. 4366597, Applied Biosystems, Waltham, MA, USA) with 100 ng of input cell-free RNA in 20 µL total volume. Quantitative real-time PCR was conducted in triplicate in 10 µL reactions containing 5 µL of TaqMan™ Universal PCR Master Mix (No UNG, 2×), 0.5 µL of TaqMan™ Small RNA Assay (20×) for each target [hsa-miR-128-3p(002216), hsa-miR-625-3p(002432), hsa-miR-130b-5p(002114), hsa-miR-151a-5p(002642), hsa-miR-330-3p(000544), hsa-miR-323a-3p(002227), hsa-miR-142-3p(000464), and hsa-miR-16-5p(000391)], 3.5 µL nuclease-free water, and 1 µL of cDNA. Reactions were run on a QuantStudio™ 5 Real-Time PCR System (Applied Biosystems) using the conditions described previously[8]. Expression levels were normalized to hsa-miR-16-5p(000391). Relative expression was calculated using the 2^-ΔΔCT method[23].

Statistical analysis

Data were expressed as median and interquartile range. The normality of each dataset was assessed using the Shapiro–Wilk test, and homogeneity of variance was evaluated with Levene's test. For datasets meeting both assumptions, intergroup comparisons were conducted using a two-tailed Student's *t*-test. If either assumption was not satisfied, the non-parametric Mann–Whitney *U* test was applied.

The miRNA diagnostic test from each miRNA was validated by ROC curves analysis: AUC, diagnostic sensitivity and specificity. Optimal cut-off points were determined by highest sensitivity plus specificity and efficiency values.

A multivariable logistic regression model was used to assess the combined impact of molecular parameters on HCM risk in FRDA. The binary outcome variable was defined as the presence (1) or absence (0) of HCM, based on standardized clinical and echocardiographic diagnostic criteria. The model included two independent variables: the square root-transformed variables Sqrt(miR-625-3p) and Sqrt(miR-323a-3p) from expression levels of miR-323a-3p and miR-625-3p. Regression coefficients (β), standard errors (SE), and 95% confidence intervals (CI) were estimated for each predictor. Odds ratios (ORs) were calculated to quantify the strength and direction of association with HCM status. The model's discriminative performance was evaluated using the AUC. Goodness-of-fit was assessed using multiple pseudo-R^2 indices, including Tjur's R^2, McFadden's R^2, Cox–Snell's R^2, and Nagelkerke's R^2, which together provided a comprehensive measure of the model's explanatory power. Calibration was examined using the Hosmer–Lemeshow test, and model fit was further supported by a statistically significant log-likelihood ratio test comparing the final model to an intercept-only model.

All statistical analyses were conducted using GraphPad Prism version9.0. Statistical significance was defined as a two-sided p-value less than 0.05.

Results

Description of participants

Thirty-four Caucasian FRDA patients were enrolled in this study, all of whom had their diagnosis confirmed by genetic testing. Participants with neoplastic diseases and active infection were excluded. The mean age of the group was 39 years and seventeen patients were men (50%). Supplementary Table 1 shows the clinical characteristics of the patients participating in the study. 15 FRDA patients (44%) had also been diagnosed with cardiomyopathy and 9 FRDA patients (26%) suffered diabetes. The remaining participants were not diagnosed with diabetes or cardiomyopathy at the time of the study.

This study also included 34 Caucasian healthy controls with no neoplastic diseases, active infection, cardiomyopathy, heart problems, hypertension, or diabetes. Of these healthy volunteers, 17 were men (50%), and the mean age of the group was 41 years (range: 19–68 years).

Validation of the differentially expressed miRNAs by RT-qPCR

In our previous study we identified a miRNA signature to differentiate FRDA patients from healthy controls: hsa-miR-128-3p; hsa-miR-625-3p, hsa-miR-130b-5p, hsa-miR-151a-5p, hsa-miR-330-3p, hsa-miR-323a-3p, and hsa-miR-142-3p[8]. We evaluated this signature in this new cohort of patients and our results showed that 5 miRNAs (miR-323a-3p, miR-128-3p, and miR-625-3p, miR-151a-5p, and miR-330-3p) were also overrepresented in this new cohort of FRDA patients compared to controls (Fig. 1, p-values shown in Fig. 1 are unadjusted). To account for multiple comparisons across the seven targeted miRNAs, we applied the Benjamini–Hochberg false discovery rate (FDR) correction ($\alpha = 0.05$). All five miRNAs remained statistically significant after FDR adjustment, confirming their robust upregulation in FRDA plasma (Supplementary Table 2). In contrast, the remaining two miRNAs (hsa-miR-130b-5p and hsa-miR-142-3p) showed non-significant trends toward upregulation following correction.

Phenotypic characterization of FRDA patients according to miRNA expression

To better understand the association between microRNA expression and disease severity in FRDA, we performed a comparative analysis based on patient stratification according to clinically relevant comorbidities. As in our previous study[8] patients were grouped by the presence or absence of specific systemic manifestations, including cardiomyopathy and diabetes mellitus.

Given the high prevalence of glucose metabolism disturbances in FRDA, and the suggested role of miRNAs in metabolic regulation, we next evaluated whether circulating miRNA levels differed between FRDA patients with and without diabetes mellitus. Patients were stratified based on clinical diagnosis of diabetes. We observed

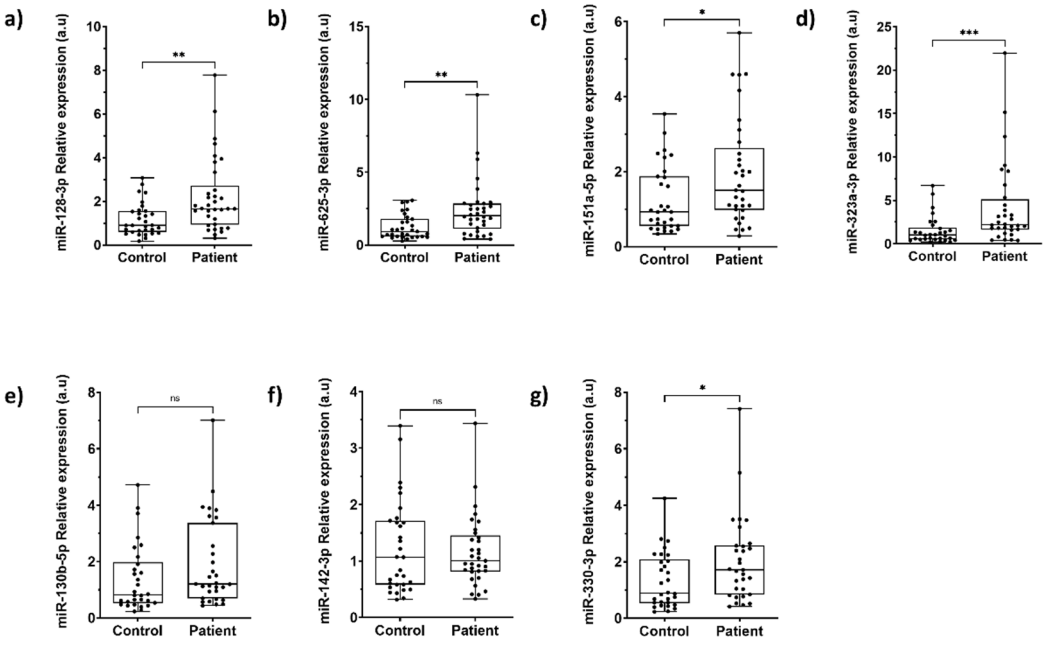

Fig. 1. Relative expression levels of the miRNAs with different representation found in plasma of FRDA patients compared to healthy control participants. Box plot of plasma levels of (**a**) hsa-miR-128-3p; (**b**) hsa-miR-625-3p, (**c**) hsa-miR-130b-5p, (**d**) hsa-miR-151a-5p, (**e**) hsa-miR-330-3p, (**f**) hsa-miR-323a-3p, and (**g**) hsa-miR-142-3p in healthy participants (Controls) (n=34) and FRDA patients (n=34). Expression levels of the miRNAs were normalized to miR-16-5p. The lines inside the boxes denote the medians. The boxes mark the interval between the 25th and 75th percentiles. The whiskers denote the interval between the 10th and 90th percentiles. Filled circles indicate data points outside the 10th and 90th percentiles. Statistically significant differences were determined using Mann-Whitney tests. All P-values were two-tailed and less than 0.05 was considered statistically significant. P-values were unadjusted for multiple comparisons.

that hsa-miR-128-3p, hsa-miR-130b-5p, hsa-miR-151a-5p, hsa-miR-330-3p, and hsa-miR-142-3p were overrepresented in plasmas from FRDA patients with diabetes compared with those that did not suffer this comorbidity (Fig. 2).

Considering that HCM is one of the most frequent and life-threatening comorbidities in FRDA, we examined whether specific circulating miRNAs were differentially expressed in patients with cardiac involvement. FRDA patients were stratified according to the presence or absence of clinically diagnosed HCM. Cardiac phenotyping was available for 32 of the 34 FRDA patients based on echocardiographic data within the predefined time window, as described in the Methods. Baseline characteristics stratified by cardiomyopathy phenotype are summarized in Supplementary Table 3. The cardiomyopathy group showed an earlier disease onset (20 vs. 13 years, $p = 0.02$), consistent with the known association between early-onset FRDA and more severe cardiac involvement[24,25]. Other variables, including age, disease duration, GAA repeat size, and diabetes prevalence, were comparable between groups (all $p > 0.05$).

We found that miR-323a-3p was overrepresented in FRDA patients with clinically diagnosed HCM compared with the remaining FRDA patients as occurred in our previous study. Moreover, miR-625-3p showed low levels in those patients with cardiomyopathy compared with the rest of FRDA patients (Fig. 3).

Echocardiographic parameters

Cardiac involvement is a hallmark of FRDA, often manifesting as HCM. To characterize the cardiac phenotype in our cohort, we performed comprehensive echocardiographic assessments, focusing on structural and functional parameters. Key measurements included IVS, LVPWT, LVEDd, LVESd, and LVEF. These evaluations aimed to elucidate the extent of myocardial remodeling and functional impairment associated with FRDA. As shown in Fig. 4, IVS and LVPWT were significatively increased in those FRDA patients with HCM, while the rest of parameters did not show statistical differences.

ROC curve analysis of echocardiographic and miRNA parameters

To evaluate the potential of echocardiographic measurements and circulating miRNAs as biomarkers for cardiac involvement in FRDA, ROC curve analyses were performed. This approach allowed us to assess the discriminative power of individual echocardiographic parameters as well as significative miRNAs previously identified as deregulated in FRDA patients with HCM. The AUC, sensitivity, and specificity values were calculated to determine the diagnostic accuracy of each variable in distinguishing patients with HCM from those without cardiac involvement. Our analysis showed that miR-323a-3p, miR-625-3p, IVS, and LVPWT had a good AUC with a significative p-value (Table 1).

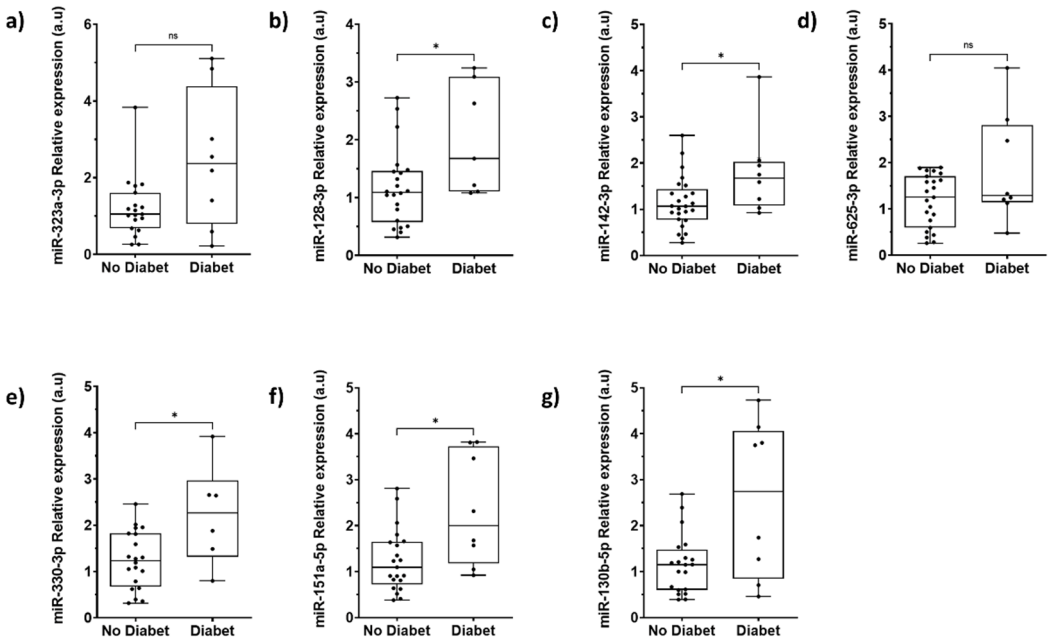

Fig. 2. Relative expression levels of the miRNAs with different representation found in plasma of FRDA patients with and without diabetes. Box plot of plasma levels of (**a**) hsa-miR-323a-3p; (**b**) hsa-miR-128-3p; (**c**) hsa-miR-142-3p; (**d**) hsa-miR-625-3p; (**e**) hsa-miR-330-3p, (**f**) hsa-miR-151a-5p, and (**g**) hsa-miR-130b-5p in FRDA patients without diabetes (No diabet; n=25) and FRDA patients with diabetes (Diabet; n=9). Expression levels of the miRNAs were normalized to miR-16-5p. The lines inside the boxes denote the medians. The boxes mark the interval between the 25th and 75th percentiles. The whiskers denote the interval between the 10th and 90th percentiles. Filled circles indicate data points outside the 10th and 90th percentiles. Statistically significant differences were determined using Mann-Whitney tests. All P-values were two-tailed and less than 0.05 was considered statistically significant.

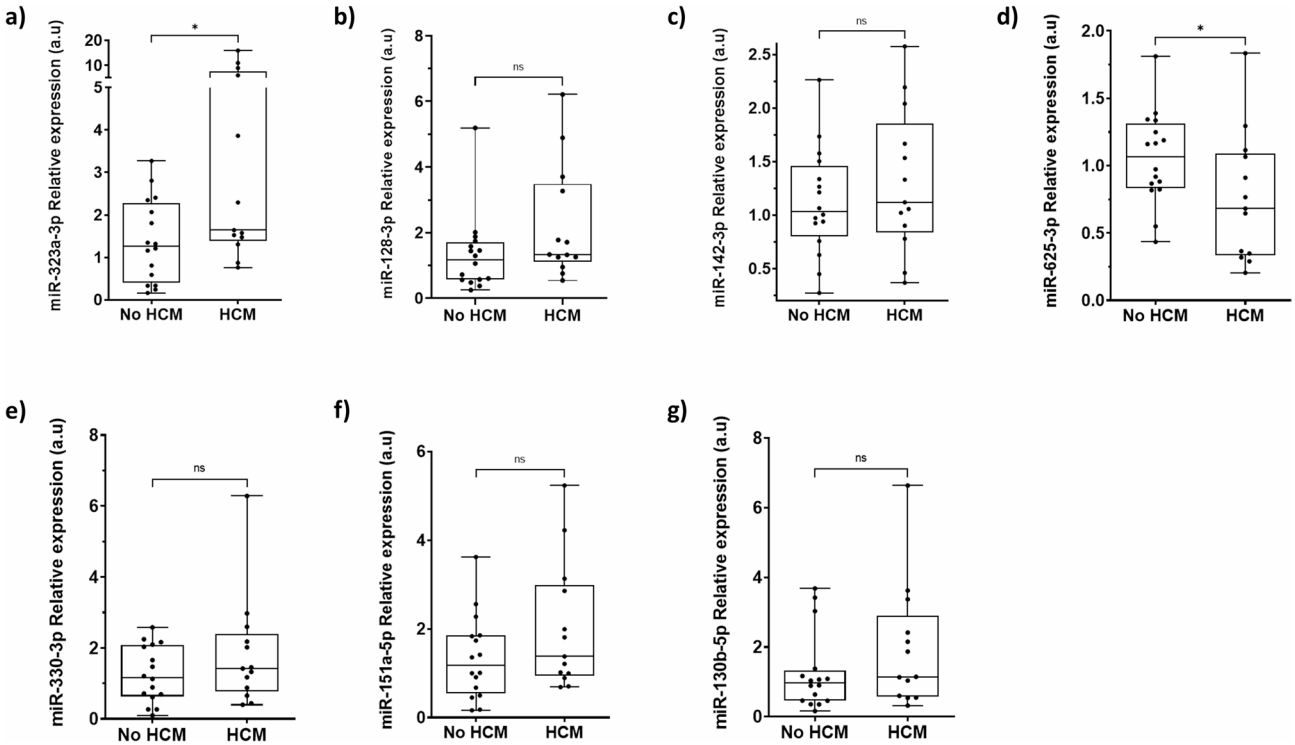

Fig. 3. Relative expression levels of the miRNAs with different representation found in plasma of FRDA patients with and without cardiomyopathy. Box plot of plasma levels of (**a**) hsa-miR-323a-3p; (**b**) hsa-miR-128-3p; (**c**) hsa-miR-142-3p; (**d**) hsa-miR-625-3p; (**e**) hsa-miR-330-3p, (**f**) hsa-miR-151a-5p, and (**g**) hsa-miR-130b-5p in FRDA patients without cardiomyopathy (No Cardio; n=17) and FRDA patients with cardiomyopathy (Cardio; n=15). Expression levels of the miRNAs were normalized to miR-16-5p. The lines inside the boxes denote the medians. The boxes mark the interval between the 25th and 75th percentiles. The whiskers denote the interval between the 10th and 90th percentiles. Filled circles indicate data points outside the 10th and 90th percentiles. Statistically significant differences were determined using Mann-Whitney tests. All P-values were two-tailed and less than 0.05 was considered statistically significant.

Multivariable analysis

To explore the combined predictive value of molecular parameters in the identification of cardiomyopathy in FRDA patients, a multivariable logistic regression model was developed. The model included the square root-transformed variables (miR-625-3p) and Sqrt(miR-323a-3p).

The regression coefficients (β), standard errors (SE), and 95% confidence intervals (CI) for each predictor are presented in Table 2. Sqrt(miR-323a-3p) showed a positive association with cardiomyopathy (β = 2.255), suggesting that higher values may be associated with increased risk, though this strong trend did not reach statistical significance (p = 0.053). Sqrt(miR-625-3p) demonstrated a negative association with the outcome (β=−5.086), potentially indicating a protective effect with statistical significance (p = 0.042).

The odds ratios (OR) derived from the regression model further illustrate the potential impact of each variable. Every unit increase in √(323a-3p) multiplied the odds of HCM by a factor of 9.53 whereas the same increment in √(miR-625-5p) divided the odds by ≈ 170.

The multivariable logistic regression model exhibited strong overall performance in discriminating between FRDA patients with and without HCM. The multivariable model yielded an AUC of 0,8117 (95% CI 0.6438 to 0.9796, p = 0.0086), suggesting promising discriminative performance despite the wide confidence interval, which reflects sample size limitations (Supplementary Fig. 1). A cut-off value of 0.3981 yielded a sensitivity of 72.7% and a specificity of 71.4%.

Model quality statistics supported the relevance of the two-marker combination. Compared with the intercept-only model, the residual deviance fell from 34.3 to 25.9 and the corrected Akaike Information Criterion (AICc) from 36.5 to 33.1; the likelihood-ratio test confirmed a significant improvement in fit (G^2=8.39, df = 2, P = 0.015). Goodness-of-fit by Hosmer–Lemeshow was satisfactory (χ^2=3.97, P = 0.860), indicating no detectable miscalibration. Pseudo-R^2 indices showed that the model accounted for approximately 24% to 38% of the variance associated with HCM status (Tjur = 0.2922; McFadden = 0.2447; Cox-Snell = 0.2851; Nagelkerke = 0.3820).

Together, these findings show promising predictive potential, suggesting the model may assist in identifying FRDA patients at increased risk of cardiomyopathy. However, further validation in larger cohorts is needed to confirm its utility.

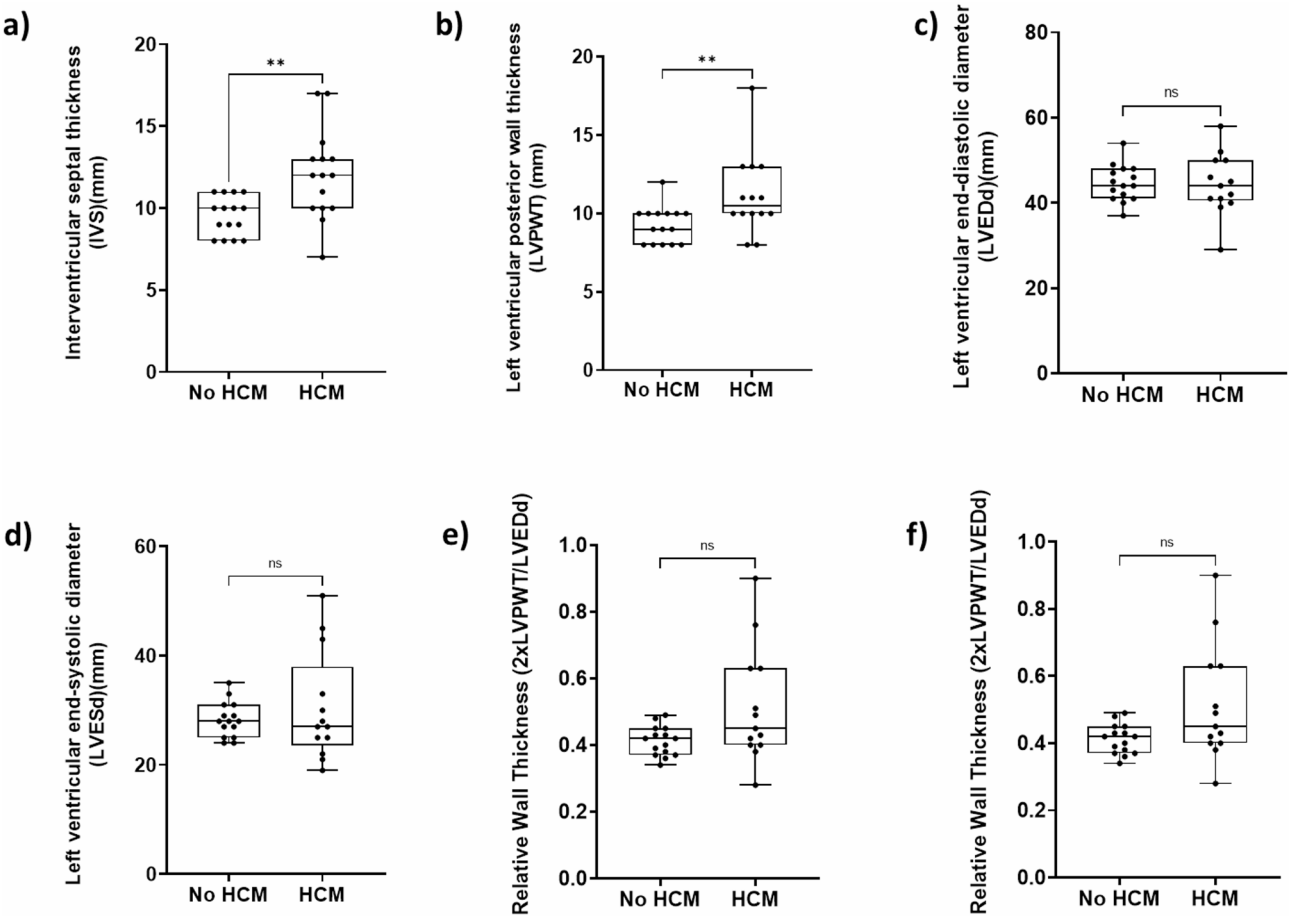

Fig. 4. Echocardiographic parameters in FRDA patients with and without hypertrophic cardiomyopathy. Dot plots show (**a**) interventricular septal thickness (IVS), (**b**) left ventricular posterior wall thickness (LVPWT), (**c**) left ventricular end-diastolic diameter (LVEDd), (**d**) end-systolic diameter (LVESd), (**e**) ejection fraction (LVEF), and (**f**) Relative Wall Thickness (RWT) in FRDA patients without cardiomyopathy (No Cardio; n=17 – 15) and FRDA patients with cardiomyopathy (Cardio; n=15 – 13). Sample sizes vary across panels, as each parameter was analyzed using all available data, and patients without a recorded measurement were excluded from the corresponding analysis. The lines inside the boxes denote the medians. The boxes mark the interval between the 25th and 75th percentiles. The whiskers denote the interval between the maximum and minimum values. Filled circles indicate data points outside the 10th and 90th percentiles. Statistically significant differences were determined using Mann-Whitney tests. All P-values were two-tailed and less than 0.05 was considered statistically significant.

miRNA	AUC	Standard error	95% CI	*p*-value	Fold change optimal cut-off value	Sensitivity (%)	Specificity (%)
miR-323a-3p	0.726	0.09	0.546, 0.912	0.039*	> 1.41	76.92	62.50
miR-625-3p	0.731	0.09	0.535, 0.927	0.035*	< 0.91	69.54	62.50
LVEF	0.513	0.12	0.286, 0.740	0.905	< 64.5	57.14	47.06
LVEDd	0.513	0.12	0.286, 0.740	0.908	> 44.50	53.85	46.67
LVESd	0.523	0.12	0.291, 0.754	0.836	< 28.5	61.54	40.00
IVS	0,809	0.08	0.645, 0,972	0.004*	> 11.5	60.00	100.00
LVPWT	0.771	0.09	0.594, 0.949	0.010*	> 11.5	28.57	93.33
RWT	0.703	0.10	0.500, 0.905	0.070	> 0.4250	61.54	60.00

Table 1. Area under ROC curves for diagnosis of hypertrophic cardiomyopathy in FRDA patients. Interventricular septal thickness (IVS), left ventricular posterior wall thickness (LVPWT), left ventricular end-diastolic diameter (LVEDd), left ventricular end-systolic diameter (LVESd), ejection fraction (LVEF), Relative Wall Thickness (RWT), area under the curve (AUC) and confidence interval (CI). * Indicates significative p-value.

Variable	β Coefficient	Standard Error	Odds Ratio (OR)	95% CI	*p*-value
Intercept	1.559	2.218	4.947	−2.656 to 6.386	0.4710
Sqrt (miR-323a-3p)	2.255	1.164	9.532	0.3743 to 5.008	0.0527
Sqrt (miR-625-3p)	−5.086	2.495	0.006182	−10.88 to −0.7345	0.0415*

Table 2. Area under ROC curves for diagnosis of hypertrophic cardiomyopathy in FRDA patients. The square root-transformed variables (Sqrt) for miR-323a-3p and miR-625-3p expression levels, Confidence interval (CI). * Indicates significative p-value.

Discusion

Validation of miRNA biomarker panel

This study expands on our earlier report of a seven-miRNA plasma signature in FRDA patients[8] by validating five components of that panel (miR-323a-3p, miR-128-3p, miR-625-3p, miR-151a-5p and miR-330-3p) in an independent, age- and sex-matched cohort. In contrast, miR-130b-5p and miR-142-3p did not show differential expression in this independent cohort. This discrepancy may reflect cohort-specific variability and underlying biological heterogeneity, particularly given the multicenter design of the validation cohort. In addition, technical factors inherent to multicenter studies, such as minor differences in pre-analytical sample handling or processing, may affect the detection of these specific miRNAs. These findings underscore the importance of external validation to identify the most robust and reproducible biomarkers across diverse clinical settings. Beyond simple replication, we show that two of these transcripts (miR-323a-3p and miR-625-3p) stratify patients according to the presence of HCM and that their combined use in a parsimonious logistic model confers promising discriminative performance when echocardiographic markers alone begin to lose sensitivity. Unlike the original single-center study, the present work recruited genetically confirmed patients from two independent hospitals and used matched healthy controls, thereby introducing greater clinical and geographic diversity. The reproducibility of the miR-323a-3p signal across centers, together with the complementary inverse pattern of miR-625-3p, strengthens the evidence that this dyad represents a robust and generalizable biomarker of cardiac involvement in FRDA.

In addition to stratifying cardiac involvement, several miRNAs from our panel, most notably miR-128-3p, miR-130b-5p, miR-151a-5p, and miR-330-3p, were significantly overexpressed in FRDA patients with diabetes ($P < 0.05$), suggesting that these markers may also reflect metabolic comorbidity and could inform integrated risk assessment for FRDA multisystem manifestations. Future studies should evaluate correlations between these miRNA levels and measures of glycemic control (e.g., HbA1c) or insulin resistance, as well as associations with disease duration and glucose-lowering therapy status, to elucidate their potential as biomarkers metabolic comorbidity in FRDA.

The confirmation of our 2017 panel strengthens the notion that dysregulated miRNA expression is a stable feature of FRDA pathophysiology, rather than a cohort-specific artefact[8]. Notably, previous studies have reported distinct miRNA signatures associated with disease progression and multisystem involvement in FRDA. A recent study in 2024 identified miR-26a-5p and miR-15a-5p as significantly correlated with cerebellar volume, spinal cord morphology, and left ventricular mass, suggesting that these miRNAs may play dual roles in neurodegeneration and cardiac hypertrophy[14]. Similarly, an earlier study in 2018 highlighted the diagnostic potential of miR-223-3p, miR-29a-3p, and miR-21-5p, which were associated with pancreatic and neuromuscular dysfunction, reinforcing the systemic nature of the disease[15]. Moreover, in a recent study of the same group they combined miR-148a-3p and miR-223-3p (AUC = 0.86, $n = 32$) to distinguish FRDA patients from controls, but did not stratify cardiac phenotype[16].

Taken together, the results position circulating miRNAs as accessible, organ-specific biomarkers capable of complementing traditional imaging in routine FRDA care and in clinical-trial enrichment.

Clinical performance and diagnostic utility

The clinical diagnosis of cardiomyopathy in our cohort was confirmed with the echocardiographic parameters following criteria mentioned in methods section.

Protein-based biomarkers explored in FRDA thus far, such as high-sensitivity troponin-T, troponin-I, and the collagen turnover marker CTX-I, have provided only modest associations with hypertrophy or fibrosis, and rarely include ROC-based discrimination. For instance, elevated troponin-I levels have been detected in approximately one-third of patients, but with limited predictive accuracy for dysfunction[26]. Similarly, CTX-I levels were found to be higher on average in FRDA, but without clinically useful thresholds[27].

In contrast, our multi-analyte microRNA model yielded robust diagnostic performance for hypertrophic cardiomyopathy in FRDA (AUC = 0.84; sensitivity 80%; specificity 71.4%), comparing favorably with traditional protein biomarkers and paralleling the performance of top miRNA panels reported in other cardiovascular conditions such as acute myocardial infarction (AUC ≥ 0.90)[28,29]. Beyond diagnostic accuracy, circulating miRNAs offer practical advantages: RT-qPCR provides a standardized, reproducible workflow with less operator dependence than echocardiography, while also capturing upstream molecular perturbations that may precede structural remodeling. This approach enables stratification of FRDA patients into high- and low-risk groups, supporting biomarker-guided surveillance strategies similar to those validated in other chronic diseases. Importantly, the integration of molecular biomarkers into clinical assessment aligns with recent guideline recommendations promoting earlier, mechanism-based interventions[11].

Mechanistic insights

Several diabetes-associated miRNAs in our panel (miR-128-3p, miR-130b-5p, miR-151a-5p, and miR-330-3p) regulate metabolic pathways, particularly insulin signaling and lipid metabolism. miR-128-3p targets key insulin signaling genes (INSR, IRS1)[30], while miR-330-3p and miR-151a-5p correlate with glycemic control and glucose tolerance, respectively[31–33]. Although we observed differential miRNA expression between FRDA patients with and without diabetes, the absence of diabetic controls prevents assessment of whether these changes were specific to FRDA-associated diabetes or reflect general diabetes-related dysregulation. Further studies including appropriate control groups will be required to address this question.

Emerging evidence indicates that the two micro-RNAs that drive our predictive model may modulate signaling hubs central to the hypertrophic–fibrotic response in FRDA cardiomyopathy. Persistent up-regulation of miR-323a-3p and concomitant down-regulation of miR-625-3p in plasma from FRDA patients may produce a receptor-level "tilt" that amplifies canonical TGF-β signalling and dismantles a key endogenous brake, SIRT1, thereby favouring the concentric-fibrotic phenotype typical of HCM. Experimental evidence supports this mechanism by showing that miR-323a-3p promotes collagen deposition and ventricular dysfunction through the suppression of TIMP3[34], SIRT1, and TGFBR2, thereby enhancing TGF-β signalling and extracellular matrix accumulation[35]. The loss of SIRT1 further facilitates endothelial-to-mesenchymal transition (EMT) and fibrogenesis[36]. In parallel, reduced miR-625-3p expression increases TGFBR1 (ALK5) levels, allowing non-canonical TGF-β signalling to persist even when TGFBR2 is limited[37]. Together, these changes sustain Smad2/3 activation and reinforce the profibrotic response characteristic of pathological cardiac remodelling.

The clinical relevance of circulating miR-323a-3p and miR-625-3p depends on whether their plasma levels reflect myocardial expression. Although these miRNAs lack direct myocardial validation, a cardiac contribution is plausible, as cardiomyocytes and fibroblasts are known to release miRNAs into the circulation, often packaged in exosome-enriched vesicles carrying heart-derived material under hemodynamic stress. Thus, the inverse plasma pattern observed may relate to intracardiac molecular changes, but this remains speculative without direct myocardial evidence.

Study limitations

This study has several important limitations. First, normalization of circulating miRNA levels was performed using a single endogenous control (miR-16-5p); this choice was deliberate, however, because our primary aim was to replicate the analytical framework of our previous report and evaluate the signature in an independent cohort using identical methodology[8]. Employing the same reference miRNA facilitates direct comparability between studies and reduces method-related heterogeneity, but reliance on one normalizer may not fully capture technical or biological variability. To improve normalization robustness, future work should incorporate multiple endogenous controls, such as combining miR-16-5p with miR-93-5p or miR-191-5p[38]. Alternatively, emerging technologies like digital PCR could be used to achieve absolute quantification, thereby circumventing the reliance on reference genes[39].

Second, the modest sample size ($n = 34$ per group), inherent to studying a rare disease such as FRDA, limits statistical power and external generalizability. We addressed this by applying strict inclusion criteria, conservative analyses, and internal validation, but larger multi-center prospective cohorts with longitudinal sampling will be needed to confirm these results and better define how miRNA changes relate to cardiac remodeling.

Third, our cohort was limited to individuals of Caucasian ancestry. Given the markedly higher prevalence of Friedreich's ataxia in populations of European descent and its rarity in other ethnic groups[40], this may further limit the generalizability of our findings. Future studies, including more diverse populations will be necessary to determine whether these miRNA alterations were consistent across different ethnic backgrounds.

Fourth, variability in the timing between echocardiographic assessment and biomarker sampling should be acknowledged. Although a maximum interval of 18 months was applied, reflecting real-world clinical practice in Friedreich's ataxia, this exceeds the 12-month interval recommended for prospective screening and may introduce minor temporal misclassification, particularly in early or borderline disease stages. However, given the slow progression of cardiac remodeling in this condition, the clinical impact of this limitation is likely limited, and only a minimal number of cases would have been excluded under a stricter 12-month threshold.

Finally, the Hosmer–Lemeshow goodness-of-fit test indicated adequate model calibration ($p = 0.70$); however, this finding should be interpreted with caution given the known limitations of this test in small samples, where it may lack sufficient power to detect miscalibration. Larger validation studies will be required to confirm model performance and calibration.

Clinical implications and future directions

Our miRNA panel shows strong potential for improving risk stratification in FRDA by identifying individuals at increased risk of developing cardiomyopathy. Evidence from cardiovascular medicine, including heart transplantation studies, demonstrates that circulating miRNAs can detect pathological changes before structural or functional damage becomes apparent[41]. Applying similar longitudinal approaches in FRDA, through serial sampling and echocardiographic follow-up, could determine the temporal relationship between miRNA alterations, wall thickening, and cardiac dysfunction. Such strategies would support precision monitoring, enabling intensified surveillance for high-risk patients while minimizing unnecessary testing in low-risk individuals.

For clinical implementation, standardized, validated diagnostic kits are needed. Guidelines for circulating miRNA biomarker studies stress the importance of robust reference controls, replication, and assay reproducibility. Prior success with miRNA assays in non-FRDA cohorts supports the feasibility of translation into clinical settings.

Finally, integrating miRNA data with other molecular and imaging markers within multi-omic risk models may further improve prediction and inform therapeutic timing. With evolving emphasis in precision medicine, such combined approaches could help intervene earlier in FRDA patients, before irreversible cardiac remodeling occurs as it happens nowadays.

Conclusions

This study independently validates a circulating miRNA signature in FRDA and supports its value for hypertrophic cardiomyopathy risk stratification. A two-miRNA panel (miR-323a-3p and miR-625-3p) showed strong diagnostic performance, surpassing conventional protein biomarkers and complementing echocardiography. Plasma miRNA measurement via standardized RT-qPCR appears feasible for clinical use. These findings highlight the potential of molecular biomarkers to improve early cardiac detection and individualized monitoring in FRDA. Prospective, multi-center longitudinal studies will be crucial to advance these miRNA markers toward validated diagnostic tools and future integration into clinical guidelines.

Data availability

The high-throughput dataset from the original discovery cohort is available in GEO under accession number GSE105052. In the present study, selected miRNAs were measured by RT-qPCR in an independent cohort; no new high-throughput datasets were generated. RT-qPCR data are available from the corresponding author upon reasonable request.

Received: 3 February 2026; Accepted: 24 April 2026
Published online: 13 May 2026

References

1. Harding, A. E. Friedreich's ataxia: A clinical and genetic study of 90 families with an analysis of early diagnostic criteria and intrafamilial clustering of clinical features. *Brain* **104**(3), 589–620 (1981).
2. Pandolfo, M. Friedreich ataxia: The clinical picture. *J. Neurol.* **256**(Suppl 1), 3–8. https://doi.org/10.1007/s00415-009-1002-3 (2009).
3. Korner, A. & Barta, L. [Association of diabetes mellitus with Friedreich's ataxia]. *Orv. Hetil.* **124**(23), 1391–2 (1983).
4. Cady, R. B. & Bobechko, W. P. Incidence, natural history, and treatment of scoliosis in Friedreich's ataxia. *J. Pediatr. Orthop.* **4**(6), 673–6 (1984).
5. Harding, A. E. & Hewer, R. L. The heart disease of Friedreich's ataxia: A clinical and electrocardiographic study of 115 patients, with an analysis of serial electrocardiographic changes in 30 cases. *Q. J. Med.* **52**(208), 489–502 (1983).
6. Durr, A. et al. Clinical and genetic abnormalities in patients with Friedreich's ataxia. *N. Engl. J. Med.* **335**(16), 1169–75. https://doi.org/10.1056/NEJM199610173351601 (1996).
7. Delatycki, M. B. et al. Clinical and genetic study of Friedreich ataxia in an Australian population. *Am. J. Med. Genet.* **87** (2), 168–174 (1999).
8. Seco-Cervera, M. et al. Circulating miR-323-3p is a biomarker for cardiomyopathy and an indicator of phenotypic variability in Friedreich's ataxia patients. *Sci. Rep.* **7**(1), 5237. https://doi.org/10.1038/s41598-017-04996-9 (2017).
9. Ao, X. et al. Non-coding RNAs regulating mitochondrial function in cardiovascular diseases. *J. Mol. Med. (Berl)* **101**(5), 501–26. https://doi.org/10.1007/s00109-023-02305-8 (2023).
10. Hyttinen, J. M. T., Blasiak, J. & Kaarniranta, K. Non-coding RNAs regulating mitochondrial functions and the oxidative stress response as putative targets against Age-Related Macular Degeneration (AMD). *Int. J. Mol. Sci.* https://doi.org/10.3390/ijms24032636 (2023).
11. Searles, C. D. MicroRNAs and cardiovascular disease risk. *Curr. Cardiol. Rep.* **26**(2), 51–60. https://doi.org/10.1007/s11886-023-02014-1 (2024).
12. Gentile, G. et al. Dysregulated miRNAs as biomarkers and therapeutical targets in Neurodegenerative Diseases. *J. Pers. Med.* https://doi.org/10.3390/jpm12050770 (2022).
13. Dandare, A., Khan, M. J., Naeem, A. & Liaquat, A. Clinical relevance of circulating non-coding RNAs in metabolic diseases: Emphasis on obesity, diabetes, cardiovascular diseases and metabolic syndrome. *Genes Dis.* **10**(6), 2393–413. https://doi.org/10.1016/j.gendis.2022.05.022 (2023).
14. Peluzzo, T. M. et al. Plasma miRNAs correlate with structural brain and cardiac damage in Friedreich's ataxia. *Cerebellum* **24**(1), 15. https://doi.org/10.1007/s12311-024-01766-y (2024).
15. Dantham, S., Srivastava, A. K., Gulati, S. & Rajeswari, M. R. Differentially regulated cell-free microRNAs in the plasma of Friedreich's ataxia patients and their association with disease pathology. *Neuropediatrics* **49**(1), 35–43. https://doi.org/10.1055/s-0037-1607279 (2018).
16. Vancheri, C. et al. An RNA-seq study in Friedreich ataxia patients identified hsa-miR-148a-3p as a putative prognostic biomarker of the disease. *Hum. Genomics* **18**(1), 50. https://doi.org/10.1186/s40246-024-00602-y (2024).
17. Bandiera, S. et al. Genetic variations creating microRNA target sites in the FXN 3'-UTR affect frataxin expression in Friedreich ataxia. *PLoS One* **8**(1), e54791. https://doi.org/10.1371/journal.pone.0054791 (2013).
18. Garcia-Gimenez, J. L. et al. Epigenetic biomarkers: Current strategies and future challenges for their use in the clinical laboratory. *Crit. Rev. Clin. Lab. Sci.* **54**(7–8), 529–50. https://doi.org/10.1080/10408363.2017.1410520 (2017).
19. Peiró-Chova, L. et al. The importance of biobanks in epigenetic studies A2. In *Epigenetic Biomarkers and Diagnostics* (eds García-Giménez, J. et al.) 19–35 (Academic, 2016).
20. Lang, R. M. et al. Recommendations for chamber quantification: A report from the American Society of Echocardiography's Guidelines and Standards Committee and the Chamber Quantification Writing Group, developed in conjunction with the European Association of Echocardiography, a branch of the European Society of Cardiology. *J. Am. Soc. Echocardiogr.* **18**(12), 1440–63. https://doi.org/10.1016/j.echo.2005.10.005 (2005).
21. Galderisi, M. et al. Standardization of adult transthoracic echocardiography reporting in agreement with recent chamber quantification, diastolic function, and heart valve disease recommendations: An expert consensus document of the European Association of Cardiovascular Imaging. *Eur. Heart J. Cardiovasc. Imaging.* **18**(12), 1301–10. https://doi.org/10.1093/ehjci/jex244 (2017).
22. Casale, P. N., Devereux, R. B., Alonso, D. R., Campo, E. & Kligfield, P. Improved sex-specific criteria of left ventricular hypertrophy for clinical and computer interpretation of electrocardiograms: Validation with autopsy findings. *Circulation* **75**(3), 565–72. https://doi.org/10.1161/01.cir.75.3.565 (1987).

23. Livak, K. J. & Schmittgen, T. D. Analysis of relative gene expression data using real-time quantitative PCR and the 2(-Delta Delta C(T)) method. *Methods* **25**(4), 402–8. https://doi.org/10.1006/meth.2001.1262 (2001).
24. Regner, S. R. et al. Analysis of echocardiograms in a large heterogeneous cohort of patients with Friedreich ataxia. *Am. J. Cardiol.* **109**(3), 401–5. https://doi.org/10.1016/j.amjcard.2011.09.025 (2012).
25. Rajagopalan, B. et al. Analysis of the factors influencing the cardiac phenotype in Friedreich's ataxia. *Mov. Disord.* **25**(7), 846–52. https://doi.org/10.1002/mds.22864 (2010).
26. Biener, M. et al. Diagnostic value of circulating microRNAs compared to high-sensitivity troponin T for the detection of non-ST-segment elevation myocardial infarction. *Eur. Heart J. Acute Cardiovasc. Care.* **10**(6), 653–60. https://doi.org/10.1093/ehjacc/zuaa034 (2021).
27. Pane, C. et al. The C-terminal cross-linked telopeptide of type I collagen (CTX-I) as a potential cardiomyopathy biomarker in friedreich ataxia patients. *Cerebellum* **22**(5), 1034–1038. https://doi.org/10.1007/s12311-022-01475-4 (2023).
28. Wang, B. et al. Comparison of the clinical value of miRNAs and conventional biomarkers in AMI: A systematic review. *Front. Genet.* **12**, 668324. https://doi.org/10.3389/fgene.2021.668324 (2021).
29. Wang, G. K. et al. Circulating microRNA: A novel potential biomarker for early diagnosis of acute myocardial infarction in humans. *Eur. Heart J.* **31**(6), 659–66. https://doi.org/10.1093/eurheartj/ehq013 (2010).
30. Motohashi, N. et al. Regulation of IRS1/Akt insulin signaling by microRNA-128a during myogenesis. *J. Cell Sci.* **126**(Pt 12), 2678–91. https://doi.org/10.1242/jcs.119966 (2013).
31. Pfeiffer, S. et al. Circulating miR-330-3p in late pregnancy is associated with pregnancy outcomes among lean women with GDM. *Sci. Rep.* **10**(1), 908. https://doi.org/10.1038/s41598-020-57838-6 (2020).
32. Akerman, L., Casas, R., Ludvigsson, J., Tavira, B. & Skoglund, C. Serum miRNA levels are related to glucose homeostasis and islet autoantibodies in children with high risk for Type 1 diabetes. *PLoS One* **13**(1), e0191067. https://doi.org/10.1371/journal.pone.0191067 (2018).
33. Sun, J. et al. miR-330-5p/Tim-3 axis regulates macrophage M2 polarization and insulin resistance in diabetes mice. *Mol. Immunol.* **95**, 107–13. https://doi.org/10.1016/j.molimm.2018.02.006 (2018).
34. Zhang, J. et al. MicroRNA-323a-3p promotes pressure overload-induced cardiac fibrosis by targeting TIMP3. *Cell. Physiol. Biochem.* **50**(6), 2176–87. https://doi.org/10.1159/000495059 (2018).
35. Iwata, J. et al. Modulation of noncanonical TGF-β signaling prevents cleft palate in Tgfbr2 mutant mice. *J. Clin. Invest.* **122**(3), 873–85. https://doi.org/10.1172/JCI61498 (2012).
36. Liu, Z. H. et al. SIRT1 activation attenuates cardiac fibrosis by endothelial-to-mesenchymal transition. *Biomed. Pharmacother.* **118**, 109227. https://doi.org/10.1016/j.biopha.2019.109227 (2019).
37. Ramachandran, A. et al. TGF-β uses a novel mode of receptor activation to phosphorylate SMAD1/5 and induce epithelial-to-mesenchymal transition. *eLife* https://doi.org/10.7554/eLife.31756 (2018).
38. Donati, S., Ciuffi, S. & Brandi, M. L. Human circulating miRNAs real-time qRT-PCR-based analysis: An overview of endogenous reference genes used for data normalization. *Int. J. Mol. Sci.* https://doi.org/10.3390/ijms20184353 (2019).
39. Maiocchi, S. et al. Plasma microrna quantification protocol. *Vessel Plus* https://doi.org/10.20517/2574-1209.2023.69 (2023).
40. Rossi, M. et al. Unravelling the global tapestry of genetic ataxias: Epidemiology and genetic testing approaches. *Mov. Disord.* **40**(9), 1805–20. https://doi.org/10.1002/mds.30302 (2025).
41. Kennel, P. J. et al. Longitudinal profiling of circulating miRNA during cardiac allograft rejection: A proof-of-concept study. *ESC Heart Fail.* **8**(3), 1840–9. https://doi.org/10.1002/ehf2.13238 (2021).

Acknowledgements

The authors gratefully acknowledge the INCLIVA Biobank and CIBERER Biobank (Valencia, Spain) for providing the biological samples used in this study. We also thank all participants, as well as the clinical and technical staff involved in recruitment, sample handling, and data collection.

Author contributions

Conceptualization and study design: M.S.C, JL.G.G. and FV.P.; Participant recruitment and sample collection: R.B.M., B.A.P., R.S., L. B., S. C., and P.G.C.; Formal data analysis: JS.I.C and M.S.C; Manuscript writing: JS.I.C and M.S.C.;. All authors were involved in discussions and participated in reviewing and editing the article and all approved the final version.

Funding

This research was funded by Instituto de Salud Carlos III and the European Regional Development Fund (FEDER) Proyectos de investigación en salud (PI19/01084; PI22/00507; PI25/01317) and by Federación de Ataxias de España (FEDAES) CONVOCATORIA DE AYUDAS A LA INVESTIGACIÓN.

Declarations

Ethics approval and consent to participate

Experimental protocols and methods were carried out after obtaining approval from the Biomedical Research Ethics Committee of HCUV (2022/173) and RVB (RVB21041ER) and it were conducted in accordance with the Declaration of Helsinki. All participants or their legal guardians provided written informed consent prior to inclusion.

Competing interests

JLG-G and FVP are co-founders and owns shares of EpiDisease S.L., a Spin-Off of the Consortium Center for Biomedical Network Research of the ISCIII. The remaining authors declare that the research was conducted in the absence of any commercial or financial relationship that could be construed as a potential conflict of interest.

Additional information

Supplementary Information The online version contains supplementary material available at https://doi.org/10.1038/s41598-026-50975-4.

Correspondence and requests for materials should be addressed to F.V.P. or M.S.-C.

Reprints and permissions information is available at www.nature.com/reprints.

Publisher's note Springer Nature remains neutral with regard to jurisdictional claims in published maps and institutional affiliations.

Open Access This article is licensed under a Creative Commons Attribution-NonCommercial-NoDerivatives 4.0 International License, which permits any non-commercial use, sharing, distribution and reproduction in any medium or format, as long as you give appropriate credit to the original author(s) and the source, provide a link to the Creative Commons licence, and indicate if you modified the licensed material. You do not have permission under this licence to share adapted material derived from this article or parts of it. The images or other third party material in this article are included in the article's Creative Commons licence, unless indicated otherwise in a credit line to the material. If material is not included in the article's Creative Commons licence and your intended use is not permitted by statutory regulation or exceeds the permitted use, you will need to obtain permission directly from the copyright holder. To view a copy of this licence, visit http://creativecommons.org/licenses/by-nc-nd/4.0/.

© The Author(s) 2026